Available online at www.sciencedirect.com

ScienceDirect

Proceedings of the Combustion Institute 38 (2021) 425–432

Proceedings of the Combustion Institute

www.elsevier.com/locate/proci

Impact of "missing" third-body efficiencies on kinetic model predictions of combustion properties

Mark C. Barbet [a], Michael P. Burke [a,b,*]

[a] Department of Mechanical Engineering, Columbia University, New York, NY, USA
[b] Department of Chemical Engineering, Data Sciences Institute, Columbia University, New York, NY, USA

Received 8 November 2019; accepted 7 June 2020
Available online 26 September 2020

Abstract

A kinetic sensitivity analysis of almost any combustion observable will highlight pressure-dependent reactions important to predictions. Third-body efficiencies play a critical role in pressure-dependent reactions, serving as a species-specific multiplier on the rate constant of the reference collider (M). When third-body efficiencies are specified, the typical convention is to specify third-body efficiencies for a handful of common species relative to nitrogen, argon, or helium as the reference (in large part due to insufficient data for most other species). Species without explicit specification of a third-body efficiency are implicitly assumed to have a value of 1.0 – i.e. the same as the reference collider. While the impact of values used for third-body efficiencies for commonly specified species like water or carbon dioxide is well recognized, the impact of unspecified or "missing" third-body colliders is considerably less known. Naturally, the lack of specification of third-body efficiencies for some species could conceivably yield significant prediction errors. Their impact could be especially pronounced given that many unspecified third bodies, which are likely to have more rovibrational degrees of freedom or have permanent dipole moments, may be more effective in inducing energy transfer than the monatomic or diatomic gases used as a reference. Here, we present a screening procedure to estimate the potential impact of unspecified third-body efficiencies; outline key results across an array of models, fuels, and initial conditions; and explore implications for model development, optimization, and validation. In general, we find that the impact of unspecified third-body efficiencies can be substantial – large enough to potentially contaminate parameter inference in optimization studies in some cases and resolve factor-of-three differences between models and experimental data in other cases. These results therefore have further implications for the list of relevant colliders to be considered in both future modeling and energy transfer studies.

Keywords: Third-body efficiencies; Pressure-dependent reactions; Kinetic modeling; Structural uncertainty

1. Introduction

It is well recognized that energy-transferring collisions play a key role in controlling rates of reactions critical to prediction of combustion

* Corresponding author at: Department of Mechanical Engineering, Columbia University, New York, NY, USA.
E-mail address: mpburke@columbia.edu (M.P. Burke).

https://doi.org/10.1016/j.proci.2020.06.178

observables. For example, any kinetic sensitivity analysis will typically reveal the importance of at least a few critical pressure-dependent reactions. As a result, a great deal of attention has been devoted to establishing pressure-dependent rate constants for these reactions. The importance of the mixture composition dependence of pressure-dependent reaction rates is also becoming increasingly recognized; many recent studies have been devoted to quantifying the efficiencies of various common bath gases for combustion reactions [1–8], evaluating the impact of mixture rules [9–13], and understanding the manifestations of reactive third-bodies [14–19]. This paper focuses on a relatively unexplored question as part of our group's broader quest to understand the impact of and better represent mixture dependence – the impact of unspecified third-body efficiencies.

In kinetic models, pressure-dependent reaction rate constants are often specified for a given reference collider "M" (almost always Ar, He, or N_2). These rate constants are sometimes accompanied by collider-specific third-body efficiencies which are species-specific multipliers of the rate constant of the reference collider (M) for a given species. When third-body efficiencies are specified, the typical convention is to specify efficiencies for a handful of common species (e.g. O_2, CO, H_2O, CO_2) relative to the reference (in large part due to insufficient data for most other species). The impact of the values used for third-body efficiencies of commonly specified species (e.g. H_2O, CO_2) on combustion predictions has been studied extensively (e.g. [20–28]) (though improved quantification of CO_2 and H_2O efficiencies remains an important outstanding issue). However, species without explicit specification of a third-body efficiency are implicitly assumed to have a value of 1.0 – i.e. the same as the reference collider. The impact of this assumption for unspecified third-body colliders is considerably less known.

Naturally, the lack of specification of third-body efficiencies for some species could have a significant impact on combustion predictions. Furthermore, this impact could be pronounced given that many unspecified species, which are likely to have more rovibrational degrees of freedom or may even have permanent dipole moments, may be more effective in inducing energy transfer than the monatomic or diatomic gases used as a reference. For example, Jasper and co-workers [3,4] found that methane (polyatomic) and water (polyatomic and polar) both have high rates of energy transfer compared to the typical monatomic or diatomic reference gases. Moreover, Fletcher et al. [29] found that many larger molecules are more effective at transferring energy in collisions; and Bernshtein and Oref found that collisions between large aromatic compounds were more efficient than collisions between aromatics and common diluents [30]. Furthermore, recent results from Matsugi [31] indicate that larger molecules and polar molecules tend to have high third-body efficiencies. Therefore, it appears worthwhile to quantify the impact of "missing" third-body efficiencies on model predictions of various combustion properties – a question that could have implications for model development, optimization, and/or validation as well as the list of colliders worth considering in future studies of third-body efficiencies for combustion-relevant colliders.

Here, to address this question, we present a screening procedure that estimates the potential uncertainties due to "missing" third-body efficiencies in predictions of ignition and flame behavior. Next, we present the results from this procedure across an array of kinetic models, fuels, and initial conditions (temperatures, pressures, and equivalence ratios) to identify general themes. We then highlight a few cases in depth to understand the key pairs of reactions and unspecified colliders. Finally, we explore the implications of unspecified third-body efficiencies on model development, optimization, and model validation. In general, we find that the impact of unspecified third-body efficiencies can be substantial – large enough potentially to contaminate parameter inference in optimization studies and resolve factor-of-three differences between models and experimental data. These results therefore have further implications for the list of relevant colliders to be considered in both future modeling and energy transfer studies.

2. Methods

A screening procedure was developed to estimate the impact of unspecified third-body efficiencies by simply switching the reference species to the species with the highest third-body efficiency (and re-normalizing the specified efficiencies and original reference species). The script encoding the procedure reads a kinetic model input file and, upon encountering a pressure-dependent reaction, performs the following steps:

1. Check if the reaction lists any efficiencies;
2. If efficiencies are present, find the maximum efficiency listed;
3. Multiply the pre-exponential factor for the low-pressure-limit rate constant by the maximum value (effectively switching the reference species to the species with the highest efficiency);
4. Normalize all the listed efficiencies by the maximum value (to maintain the same rate constants for each species with specified third-body efficiency). If no efficiency is listed for Ar, He, N_2, and O_2 (which are usually either the original reference collider or assumed to be the same as the original reference collider), they are all assigned

Table 1
Mechanisms used for flame speed and ignition delay screening simulations [23,33–45].

Mechanisms	Flame speed	Ignition delay
FFCM-1	✓	✓
Aramco 2.0		✓
Galway DME	✓	✓
Zhao DME	✓	✓
Li/Dryer Methanol	✓	✓
Metcalfe	✓	✓
LLNL Reduced Heptane	✓	✓
JetSurf		✓
Galway Heptane		✓
LLNL C8-C16		✓

the corresponding value for the original reference.

This script produces a modified kinetic model input file with the most effective collider as the reference collider. (Note that this procedure only examines reactions written in terms of the reference species "M" and does not consider reactions written in PLOG format or mixture rule effects [9–11], both of which may produce deviations in addition to those examined here. See Table S16 in Supplemental Material for a count of various pressure-dependent formats in each model.)

Comparisons of combustion predictions using the nominal and modified kinetic model then reveal the impact of unspecified third-body colliders. If predictions using the modified model do not deviate from those using the nominal model, the list of specified colliders is deemed sufficient for that particular combustion situation. Alternatively, if predictions using the modified model deviate significantly from those of the nominal model, sensitivity analysis is used to identify the pressure-dependent reactions responsible for the differences. (It is perhaps worth noting that the deviations found here should not be interpreted as the "true" error for not specifying third-body efficiencies for a given collider since data for most colliders and reactions are not available to evaluate a true error.) Further simulations that include one additional collider at a time for each of the sensitive pressure-dependent reactions can then be used to pinpoint the specific "missing" collider(s) in the reaction(s) responsible for the deviations.

This procedure was implemented for a variety of kinetic models, given in Table 1. Predictions (using Cantera [32]) were performed across a broad range of fuels (cf. Fig. 1), equivalence ratios (0.5 to 4.5), and pressures (1 atm to 10 atm) for laminar flame speeds and across a broad range of fuels (cf. Fig. 4), equivalence ratios (0.5 to 4.0), temperatures (500 K to 1700 K), and pressures (1 atm to 100 atm) for ignition delay times.

3. Results and discussion

3.1. Laminar flame speeds

To visualize the results across a broad array of cases for laminar flame speeds, Figs. 1 and 2 show deviations due to unspecified third-body efficiencies for various fuels and equivalence ratios. Each bar in Fig. 1 shows the range of maximum deviations across different models for a given fuel, where the lower limit of the bar indicates the maximum deviation observed for the model with the smallest maximum deviation, while the upper limit of the bar indicates the maximum deviation observed for any model; the large gap between the upper and lower limits on each bar gives an indication of the strong dependence of collider efficiency uncertainties on the kinetic model used. Each x-mark in Fig. 1 indicates the average maximum deviation across all models, which may serve as an indication of whether a particular fuel is generally affected or if only a few models are affected for that fuel. Similar results are shown in Fig. 2 for

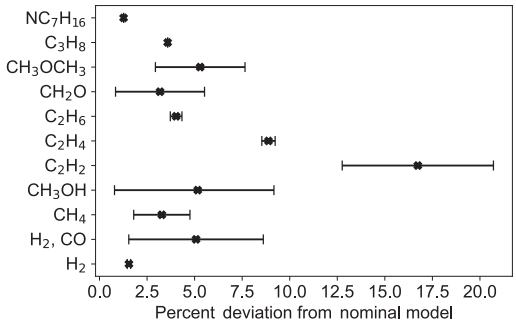

Fig. 1. The average (x-marks) and range (bars) of maximum laminar flame speed deviations found for each fuel among different models. Each bar shows the range of maximum deviations across different models for a given fuel, where the lower limit of the bar indicates the maximum deviation observed for the model with the smallest maximum deviation, while the upper limit of the bar indicates the maximum deviation observed for any model. Each x-mark indicates the average maximum deviation across all models.

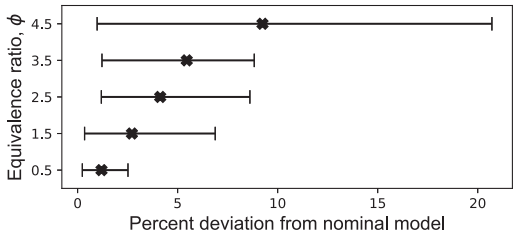

Fig. 2. The average (x-marks) and range (bars) of maximum laminar flame speed deviations found for each equivalence ratio among different models (cf. Fig. 1 caption).

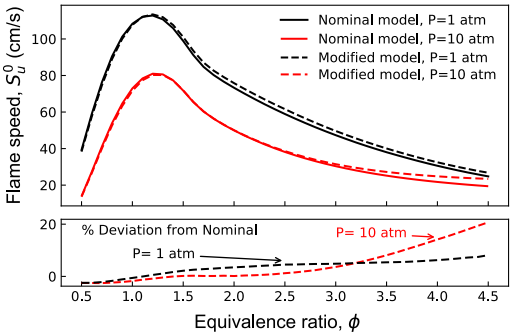

Fig. 3. Flame speed predictions for C_2H_2/air mixtures as a function of equivalence ratio for several pressures (Top) and percent deviations from the nominal model (Bottom).

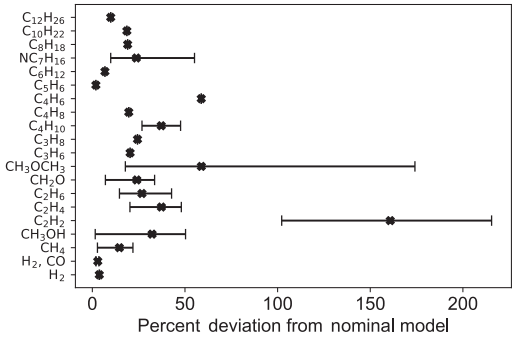

Fig. 4. The average (x-marks) and range (bars) of maximum ignition delay time deviations found for each fuel among different models (cf. Fig. 1 caption).

Table 2
For the four cases highlighted previously, this table enumerates the pressure-dependent reactions as well as the critical colliders without specified efficiencies that cause most of the deviations seen in Figs. 3, 6–8.

Reference figure	Reaction(s)	Collider
Fig. 3	CH_3 +H (+ M) ↔ CH_4 (+ M), C_2H_2 + H (+ M) ↔ C_2H_3 (+ M), HCO + M ↔ CO + H + M	C_2H_2
Fig. 6	H_2O_2 (+ M) ↔OH + OH (+ M)	CH_3OH
Fig. 7	H + C_2H_2 (+ M) ↔ C_2H_3 (+ M)	C_2H_2, C_2H_4
Fig. 8	H + C_2H_2 (+ M) ↔ C_2H_3 (+ M), H+O_2(+M)↔HO_2(+M)	C_2H_2

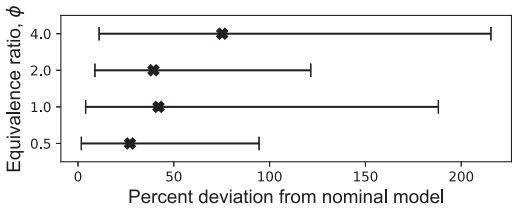

Fig. 5. The average (x-marks) and range (bars) of maximum ignition delay time deviations found for each equivalence ratio among different models (cf. Fig. 1 caption).

various equivalence ratios. As shown in Figs. 1 and 2, the largest deviations appear for smaller fuels and higher equivalence ratios – both of which correlate with higher fuel mole fractions in the fuel/air mixture and the fact that fuel molecules are often among the species without specified third-body efficiencies. While the largest deviations (∼20%) tended to occur at higher equivalence ratios than those typically considered in experimental and modeling studies, deviations up to ∼7% are found even for equivalence ratios near 1.5.

Model predictions of C_2H_2/air flame speeds shown in Fig. 3 are representative of the general trends observed. The exact results shown are for model variants based on FFCM-1 (though similar results are found for other models such as Metcalfe [23]). Here, deviations from the nominal model are largest at high equivalence ratios. Sensitivity analysis revealed a few pressure-dependent reactions responsible for the deviations, displayed in Table 2. Further simulations identified that the fuel itself, C_2H_2, was the species without a provided efficiency that was most responsible for the deviations.

3.2. Ignition delay times

To visualize the results across a broad array of cases for ignition delay times, Figs. 4 and 5 show deviations due to unspecified third-body efficiencies for various fuels and equivalence ratios across different kinetic models. Similar to the largest deviations for flame speeds, the largest deviations for ignition delay times appear for smaller fuel molecules and there is still a strong kinetic model dependence in the collider efficiencies. The trend with equivalence ratio is less pronounced for ignition delay times than for flame speeds. However, aside from the results for C_2H_2, the results show a general trend to larger deviations at high equivalence ratios (similar to that for flame speeds). Some key results and insights are discussed below for a few case studies.

Figure 6 shows ignition delay time deviations for stoichiometric and rich CH_3OH/air mixtures. The exact results shown are for model variants based on Li et al. [33] (though similar results are found for other models such as Olm et al. [46], Metcalfe [23], and Aramco 2.0 [23,35–40]). Sensitivity analysis indicated that $H_2O_2(+M) = OH + OH(+M)$ is the reaction primarily responsible for the deviation. Further simulations then identified CH_3OH as the unspecified collider responsible for the deviation. Deviations reach ∼30% for stoichiometric mixtures (where the CH_3OH mole fraction is 12.3%) and ∼50% for rich mixtures (where the CH_3OH mole fraction is 35.9%).

Similarly, Fig. 7 shows ignition delay time deviations for stoichiometric and rich C_4H_{10}/air

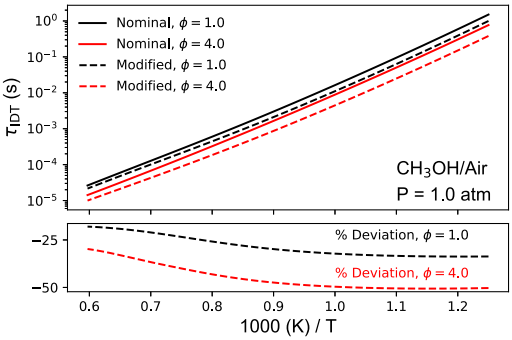

Fig. 6. Ignition delay time predictions for CH_3OH/air mixtures at several equivalence ratios (Top) and deviations from the nominal model (Bottom).

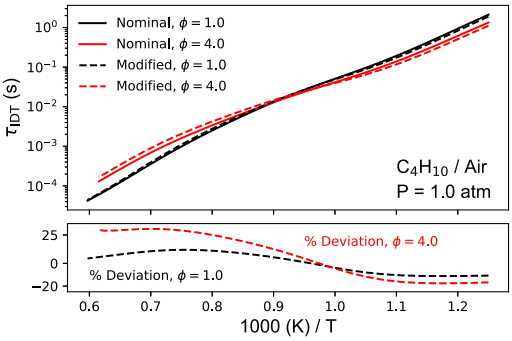

Fig. 7. Ignition delay time predictions for C_4H_{10}/air mixtures at several equivalence ratios (Top) and deviations from the nominal model (Bottom).

mixtures. The exact results shown are for model variants based on Aramco 2.0 [23,35–40]. Further analysis indicated that unspecified third-body efficiencies for $H + C_2H_2(+M) \leftrightarrow C_2H_3(+M)$ were responsible for the deviations. Interestingly, the key unspecified colliders were not the parent fuel (C_4H_{10}) but fuel fragments (C_2H_2 and C_2H_4). The importance of smaller fuel fragments (e.g. C_2H_2, C_2H_4), rather than the parent fuel, was observed for other larger fuel molecules (e.g. n-heptane). Indeed, the mole fractions of small fuel fragments can reach higher values than larger parent fuels and, consequently, the impact of unspecified efficiencies of small fuel fragments can be higher than those for the parent fuel.

The most significant deviations again were found in C_2H_2/air mixtures as shown in Fig. 8 for equivalence ratios of 1.0 and 4.0. The exact results shown are for model variants based on Aramco 2.0 [23,35–40] (similar results are found for other models such as Gimenez-Lopez et al. [47] and Metcalfe et al. [23]). The most significant deviations were found in intermediate temperature ranges. Interestingly, the maximum deviations are comparable for stoichiometric and rich mixtures even though

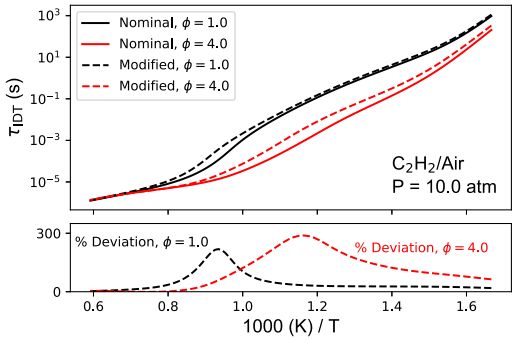

Fig. 8. Ignition delay time predictions for C_2H_2/air mixtures at several equivalence ratios (Top) and deviations from the nominal model (Bottom).

they peak at different temperatures ($\sim$1100 K for an equivalence ratio of 1.0 and $\sim$800 K for an equivalence ratio of 4.0). Further analysis identified C_2H_2 as the critical unspecified collider for $H + O_2 + M \leftrightarrow HO_2 + M$ and $C_2H_2 + H + M \leftrightarrow C_2H_3(+M)$.

Across many ignition delay time simulations, the critical unspecified collider belonged to a relatively short list of fuel fragments or fuels which exist in sufficient quantities (especially at higher equivalence ratios) to affect observables. These critical colliders and reactions for the cases highlighted above are tabulated in Table 2.

3.3. *Implications for model development, optimization, and validation*

Interestingly, the magnitude of the deviations observed are comparable (or larger) than both (1) uncertainties in experimental measurements and (2) differences between model predictions and experimental data – differences that often motivate parameter adjustments in model development studies to match data. In such cases, differences between experimental data and model predictions may be attributed to the wrong aspects of the model in model development and/or optimization studies.

For example, for the purposes of uncertainty quantification, unspecified third-body efficiencies constitute a major structural uncertainty [49–51]. Use of experimental measurements whose predictions are impacted by these uncertainties is likely to impose false constraints on the model parameters – essentially contaminating parameter inference based on the data [53]. Interestingly, CH_3OH/air ignition delay times, which appear to be strongly affected by unspecified efficiencies, are among the targets considered in a recent optimization study [46,48]. Figure 9 shows the deviations due to unspecified efficiencies (for models from [33,46]) at the exact conditions of one of these optimization targets. Here, the estimated deviations (of $\sim$20–

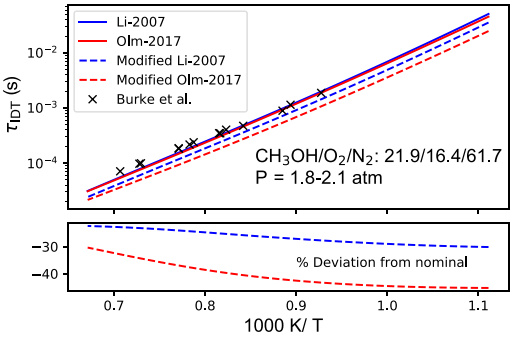

Fig. 9. Ignition delay time predictions for a CH_3OH/air mixture using models based on [33,46] compared to experimental data [48] (Top) and deviations from these nominal models (Bottom).

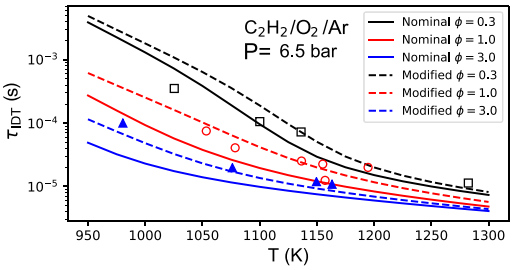

Fig. 10. Ignition delay time predictions for C_2H_2/O_2/Ar mixtures at several equivalence ratios using models based on [47] compared to experimental data [52].

50%) are larger than the experimental uncertainty ($\sim$10%).

The effects highlighted here are also of relevance to model development and validation more broadly. For example, Fig. 10 shows the impact of unspecified third-body efficiencies on predictions of C_2H_2/O_2/Ar ignition delay times based on the model of Gimenez-Lopez et al. [47] compared to experimental data [52] used to test the model. The impact of unspecified efficiencies reaches a factor of $\sim$3 and tend to improve agreement with the experimental data (at least at high equivalence ratios). In fact, use of typical values for C_2H_2 and C_2H_4 collision efficiencies (from models where they are specified) instead of those used in the algorithm here yields deviations in simulations that are lower but still significant – of similar or greater magnitude to errors reported in many ignition delay studies. These results suggest that unspecified efficiencies may contribute to the differences between model predictions and experimental data.

4. Conclusions

Results generated across a wide range of kinetic models, combustion properties, fuels, temperatures, pressures, and equivalence ratios revealed that the impact of unspecified third-body efficiencies can be substantial – reaching up to $\sim$20% for laminar flame speeds and a factor of $\sim$3 for ignition delay times.

Based on the cases explored in depth, the critical unspecified collider was usually a small fuel molecule (e.g. C_2H_2, C_2H_4) – even if the parent fuel were much larger (e.g. C_4H_{10} or C_7H_{16}) – which can be present in higher mole fractions at a given equivalence ratio. While the largest deviations were observed for small fuels (e.g. C_2H_2, CH_3OH), even larger fuels (e.g. C_4H_{10} or C_7H_{16}) were found to exhibit significant deviations (e.g. up to $\sim$50% for ignition delay times). Similarly, deviations usually increased with equivalence ratio, where fuel mole fractions are higher, though deviations even for lean and stoichiometric mixtures are still significant.

Altogether, the present results suggest that uncertainties in unspecified third-body efficiencies could be alleviated through consideration of a small list of common fuels and fuel fragments (e.g. CH_3OH, C_2H_2, C_2H_4) in future kinetic modeling studies. A major impediment to reducing this uncertainty is that data for most collider and fuel pairs are not currently available. Clearly, future studies characterizing third-body efficiencies would be highly worthwhile and the present study would suggest that the list of commonly considered colliders be expanded to include more small fuel fragments. In the meantime, unspecified third-body efficiencies can be considered to constitute a major uncertainty in the model structure worth considering in future model development, optimization, and validation studies. The present procedure may serve as a useful tool to estimate potential deviations due to unspecified third-body efficiencies.

Similarly, since most unspecified species are likely to have higher efficiencies than the usual monatomic or diatomic reference species, it could be argued that using the species with the highest efficiency as the reference species (i.e. the modified models produced by the present procedure) may actually be more accurate.

While the present paper is focused on one specific aspect of uncertainties due to collider effects – the impact of unspecified third-body efficiencies – there are of course a number of aspects of collisional effects that require further attention. These include (among others): (1) improved characterization of energy-transfer parameters (a la [1–8]) especially for common diluents, H_2O, CO_2, and, as per the present study, common fuels and fuel fragments across many reactions; (2) ability to specify temperature- and pressure-dependent third-body efficiencies in combustion codes (without sacrificing ability to represent mixture dependence accurately, cf. [9]); (3) lack of collider effects included for most reactions whose rate constants are written in PLOG format; (4) development and incorpora-

tion of improved mixture rules [9–13] in combustion codes to better represent the mixture dependence of rate constants for pressure-dependent reactions; and (5) improved characterization of and improved rate laws for chemically termolecular reactions that manifest from reactive collisions of the energized intermediates that mediate pressure-dependent reactions [14–19]. In general, for many reasons, the treatment of mixture dependence has not yet reached the same level of fidelity as treatments of temperature and pressure dependence in chemical kinetics.

Declaration of Competing Interest

The authors declare that they have no known competing financial interests or personal relationships that could have appeared to influence the work reported in this paper.

Acknowledgments

The authors gratefully acknowledge support from the National Science Foundation through a grant from the Computational and Data-Enabled Science and Engineering (CDS&E) program (Award #1761491).

Supplementary material

Supplementary material associated with this article can be found, in the online version, at doi:10.1016/j.proci.2020.06.178.

References

[1] R.X. Fernandes, K. Luther, J. Troe, V.G. Ushakov, *Phys. Chem. Chem. Phys.* 10 (2008) 4313–4321.
[2] A.W. Jasper, J.A. Miller, *J. Phys. Chem. A* 113 (2009) 5612–5619.
[3] A.W. Jasper, J.A. Miller, *J. Phys. Chem. A* 115 (2011) 6438–6455.
[4] A.W. Jasper, J.A. Miller, S.J. Klippenstein, *J. Phys. Chem. A* 117 (47) (2013) 12243–12255.
[5] A.W. Jasper, C.M. Oana, J.A. Miller, *Proc. Combust. Inst.* 35 (2015) 197–204.
[6] J. Shao, R. Choudhary, A. Susa, D.F. Davidson, R.K. Hanson, *Proc. Combust. Inst.* 37 (2019) 145–152.
[7] R. Choudhary, J.J. Girard, J. Shao, D.F. Davidson, R.K. Hanson, *Combust. Flame* 203 (2019) 265–278.
[8] A.W. Jasper, *Int. J. Chem. Kinet.* 52 (6) (2020) 387–402.
[9] M.P. Burke, R. Song, *Proc. Combust. Inst.* 36 (2017) 245–253.
[10] L. Lei, M.P. Burke, *Proc. Combust. Inst.* 37 (2019) 355–362.
[11] L. Lei, M.P. Burke, *J. Phys. Chem. A* 123 (2019) 631–649.
[12] L. Lei, M.P. Burke, *Combust. Flame* 213 (2020) 467–474.
[13] L. Lei, M.P. Burke, *Proc. Combust. Inst.* (2020), doi:10.1016/j.proci.2020.06.187.
[14] M.P. Burke, C.F. Goldsmith, Y. Georgievskii, S.J. Klippenstein, *Proc. Combust. Inst.* 35 (1) (2015) 205–213.
[15] M.P. Burke, S.J. Klippenstein, *Nat. Chem.* 9 (2017) 1078–1082.
[16] M.C. Barbet, K. McCullough, M.P. Burke, *Proc. Combust. Inst.* 37 (2019) 347–354.
[17] A.W. Jasper, R. Sivaramakrishnan, S.J. Klippenstein, *J. Chem. Phys.* 150 (114112) (2019).
[18] L. Lei, M.P. Burke, *Proc. Combust. Inst.* (2020), doi:10.1016/j.proci.2020.06.385.
[19] R.E. Cornell, M.C. Barbet, M.P. Burke, *Proc. Combust. Inst.* (2020), doi:10.1016/j.proci.2020.06.354.
[20] G. Dixon-Lewis, *Proc. R. Soc. Lond. A* 317 (1970) 235–263.
[21] G. Dixon-Lewis, J.B. Greenberg, F.A. Goldsworthy, *Symp. (Int.) Combust.* 15 (1975) 717–730.
[22] S. Davis, A. Joshi, H. Wang, F. Egolfopoulos, *Proc. Combust. Inst.* 30 (2005) 1283–1292.
[23] W.K. Metcalfe, S.M. Burke, S.S. Ahmed, H.J. Curran, *Int. J. Chem. Kinet.* 45 (10) (2013) 638–675.
[24] P. Sabia, M. Lubrano Lavadera, P. Giudicianni, G. Sorrentino, R. Ragucci, M. de Joannon, *Combust. Flame* 162 (3) (2015) 533–543.
[25] O. Park, P.S. Veloo, D.A. Sheen, Y. Tao, F.N. Egolfopoulos, H. Wang, *Combust. Flame* 172 (2016) 136–152.
[26] H.J. Curran, *Proc. Combust. Inst.* 37 (2019) 57–81.
[27] A.E. Long, R.L. Speth, W.H. Green, *Combust. Flame* 202 (2019) 318–333.
[28] M.P. Burke, M. Chaos, F.L. Dryer, Y. Ju, *Combust. Flame* 157 (2010) 618–631.
[29] F.J. Fletcher, B.S. Rabinovitch, K.W. Watkins, D.J. Locker, *J. Phys. Chem.* 70 (9) (1966) 2823–2833.
[30] V. Bernshtein, I. Oref, *Isr. J. Chem.* 47 (2007) 205–214.
[31] A. Matsugi, *J. Phys. Chem. A* 123 (2019) 764–770.
[32] D.G. Goodwin, H.K. Moffat, R.L. Speth, Cantera: An Object-Oriented Software Toolkit for Chemical Kinetics, Thermodynamics, and Transport Processes, 2017. Version 2.3.0.
[33] J. Li, Z. Zhao, A. Kzakov, M. Chaos, F.L. Dryer, J.J. Scire, *Int. J. Chem. Kinet.* 39 (2007) 109–136.
[34] G. Smith, Y. Tao, H. Wang, Foundational Fuel Chemistry Model Version 1.0 (FFCM-1.0) (2016).
[35] Y. Li, C.-W. Zhou, K.P. Somers, K. Zhang, H.J. Curran, *Proc. Combust. Inst.* 36 (1) (2017) 403–411.
[36] C.-W. Zhou, Y. Li, E. O'Connor, K.P. Somers, S. Thion, C. Keesee, O. Mathieu, E.L. Petersen, T.A. DeVerter, M.A. Oehlschlaeger, G. Kukkadapu, C.-J. Sung, M. Alrefae, F. Khaled, A. Farooq, P. Dirrenberger, P.-A. Glaude, F. Battin-Leclerc, J. Santner, Y. Ju, T. Held, F.M. Haas, F.L. Dryer, H.J. Curran, *Combust. Flame* 167 (2016) 353–379.
[37] U. Burke, W.K. Metcalfe, S.M. Burke, K.A. Heufer, P. Dagaut, H.J. Curran, *Combust. Flame* 165 (2016) 125–136.
[38] S.M. Burke, U. Burke, R. McDonagh, O. Mathieu, I. Osorio, C. Keesee, A. Morones, E.L. Petersen, W. Wang, T.A. DeVerter, M.A. Oehlschlaeger, B. Rhodes, R.K. Hanson, D.F. Davidson, B.W. Weber, C.-J. Sung, J. Santner, Y. Ju, F.M. Haas, F.L. Dryer, E.N. Volkov, E.J. Nilsson, A.A. Konnov, M. Alrefae, F. Khaled, A. Farooq, P. Dirrenberger,

P.-A. Glaude, F. Battin-Leclerc, H.J. Curran, *Combust. Flame* 162 (2) (2015) 296–314.
[39] S.M. Burke, W. Metcalfe, O. Herbinet, F. Battin-Leclerc, F.M. Haas, J. Santner, F.L. Dryer, H.J. Curran, *Combust. Flame* 161 (11) (2014) 2765–2784.
[40] A. Kéromnès, W.K. Metcalfe, K.A. Heufer, N. Donohoe, A.K. Das, C.-J. Sung, J. Herzler, C. Naumann, P. Griebel, O. Mathieu, M.C. Krejci, E.L. Petersen, W.J. Pitz, H.J. Curran, *Combust. Flame* 160 (6) (2013) 995–1011.
[41] U. Burke, K.P. Somers, P. O'Toole, C.M. Zinner, N. Marquet, G. Bourque, E.L. Petersen, W.K. Metcalfe, Z. Serinyel, H.J. Curran, *Combust. Flame* 162 (2) (2015) 315–330.
[42] Z. Zhao, M. Chaos, A. Kazakov, F.L. Dryer, *Int. J. Chem. Kinet.* 40 (1) (2008) 1–18.
[43] H. Seiser, H. Pitsch, K. Seshadri, W.J. Pitz, H.J. Curran, *Proc. Combust. Inst.* 28 (2000) 2029–2037.
[44] H. Wang, E. Dames, B. Sirjean, D.A. Sheen, R. Tango, A. Violi, J.Y.W. Lai, F.N. Egolfopoulos, D.F. Davidson, R.K. Hanson, C.T. Bowman, C.K. Law, W. Tsang, N.P. Cernansky, D.L. Miller, R.P. Lindstedt, JetSurF version 2.0 (2010).
[45] K. Zhang, C. Banyon, J. Bugler, H. Curran, A. Rodriguez, O. Herbinet, F. Battin-Leclerc, C. B'Chir, K. Heufer, *Combust. Flame* 172 (2016) 116–135 .
[46] C. Olm, T. Varga, É. Valkó, H.J. Curran, T. Turányi, *Combust. Flame* 186 (2017) 45–64.
[47] J. Gimenez-Lopez, C.T. Rasmussen, H. Hashemi, M.U. Alzueta, Y. Gao, P. Marshall, C.F. Goldsmith, P. Glarborg, *Int. J. Chem. Kinet.* 48 (11) (2016) 724–738.
[48] U. Burke, W.K. Metcalfe, S.M. Burke, K.A. Heufer, P. Dagaut, H.J. Curran, *Combust. Flame* 165 (2016) 125–136.
[49] M.P. Burke, C.F. Goldsmith, S.J. Klippenstein, O. Welz, H. Huang, I.O. Antonov, J.D. Savee, D.L. Osborn, J. Zádor, C.A. Taatjes, L. Sheps, *J. Phys. Chem. A* 119 (28) (2015) 7095–7115.
[50] M.P. Burke, *Int. J. Chem. Kinet.* 48 (4) (2016) 212–235.
[51] D.A. Sheen, H. Wang, *Combust. Flame* 158 (12) (2011) 2358–2374.
[52] A.M. Tereza, V.G. Slutskii, E.S. Severin, *Russ. J. Phys. Chem. B* 3 (2009) 99–108.
[53] C.E. LaGrotta, M.C. Barbet, L. Lei, M.P. Burke, *Proc. Combust. Inst.* (2020), doi:10.1016/j.proci.2020.06.324.